Multi-objective optimization design of hybrid excitation doubly salient motor based on Taguchi method

Xiangyun Gao[1], Xiaoli Meng[2], Ao Shen, Xufei Zhang, Qiwei Wu
Dept. of Electrical Engineering
Nanjing University of Aeronautics and Astronautics, China

Abstract— **Hybrid excitation doubly salient motor (HEDSM) is suitable for aviation starter/generator because of the advantages of high-power density, high reliability and flexible control. However, the salient pole and slot structure can cause high torque ripple and serious nonlinear magnetic field distribution. In this paper, we present a multi-objective optimization design approach for the HEDSM. In order to increase the output torque of the motor and reduce the torque ripple of the motor, the Taguchi method is used to optimize parameters of the motor. The ANOVA is often used in traditional Taguchi method to analyze the data of orthogonal experiments to determine the final optimization result, but it is more suitable for single-objective optimization. Therefore, the grey relational analysis (GRA) is used instead of ANOVA to improve the Taguchi method, so as to complete the multi-objective optimization design of the motor. Finally, the simulation and analysis of characteristics for the HEDSM verifies the effectiveness of the optimization method, which enriches the rapid design and optimization methods of this kind of doubly-salient motors.**

Index Terms—HEDSM; torque; Taguchi method; GRA.

I. INTRODUCTION

Doubly salient motor (DSM) has gradually become one of the preferred motor types for aviation starter/generator due to its advantages of simple and robust structure, safety of use and high-speed operation, which has gradually attracted extensive attention and research from scholars in the field of motor at home and abroad in recent years [1]-[2].

DSM include switched reluctance motor (SRM), doubly salient permanent motor (DSPM), doubly salient electromagnetic motor (DSEM) and HEDSM. Among them, the HEDSM combines the advantages of DSPM and DSEM, which can be used for independent power generation, and electrical excitation to expand the range of regulating the air gap magnetic field, high power density, simple control, high fault tolerance, which has potential application prospects in aerospace, electric vehicles, wind power generation and other fields [3]-[5].

However, due to its fixed salient pole structure, the DSM generates large torque ripple when operating electrically. So far, the research on problem of the torque ripple for DSM has mainly focused on the structure and control strategy of the motor. In [6], advanced angle control (ACC) is adopted when the motor is running at high speed, which improves the output torque, and the two-section twisted-rotor structure is adopted to further suppress torque ripple. In [7], a three-phase six-state (TPSS) control strategy is proposed, which can effectively suppress torque ripple, improve output torque, and reduce bus reverse current through a certain angle combination. In [8], the skew slot structure is adopted to reduce the torque ripple of PMSM.

At present, there are few researches on optimization design of the parameter for DSM. Commonly used optimization design methods, such as the magnetic circuit method, are mainly enumerated and compared, which are less efficient, so intelligent algorithms are often used to optimize the design of DSM. In [9], the efficiency and torque ripple are selected as the objective function, and the initial size is multi-optimized based on the improved genetic algorithm (GA), and the multi-objective optimization design of RSM is realized.

Taguchi analysis method is a low-cost, cost-effective experimental design method, which has occupied a place in the field of optimization design for motor in recent years. In [10], the shape, thickness and embrace of permanent magnets are selected as optimization parameters, the Taguchi method is used to perform multi-objective optimization to improve efficiency of the PMSM. In [11], based on the hybrid Taguchi genetic algorithm, electromagnetic torque, torque ripple and iron loss are selected as the optimization target to optimize parameters of a hybrid excitation permanent magnet synchronous motor. However, the traditional Taguchi method is more suitable for single-objective optimization.

Therefore, the grey relational analysis (GRA) [12] is used instead of ANOVA to improve the Taguchi method. In this paper, the output torque and torque ripple are selected as the optimization targets, the air gap, stator pole

This paper is supported by the National Natural Science Foundation of China (51737006)

height, rotor pole arc, permanent magnet height and permanent magnet width of a 24/16 pole HEDSM are optimized based on the improved Taguchi method. Finally, the distribution of magnetic field and the flux-linkage, back EMF, inductance and torque characteristics of the motor are analyzed to verify the effectiveness of the method.

II. Structure and Mathematical Model of HEDSM

A. Structure

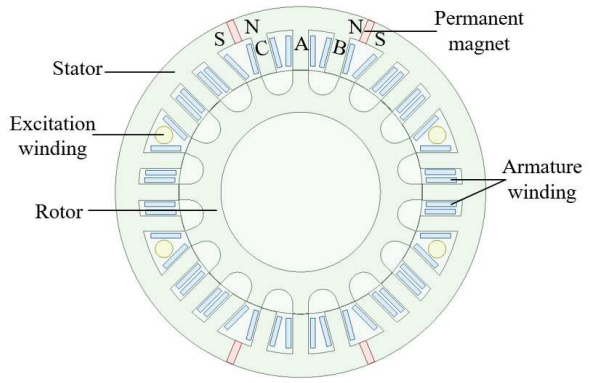

Fig. 1. The structure of 24/16-pole HEDSM

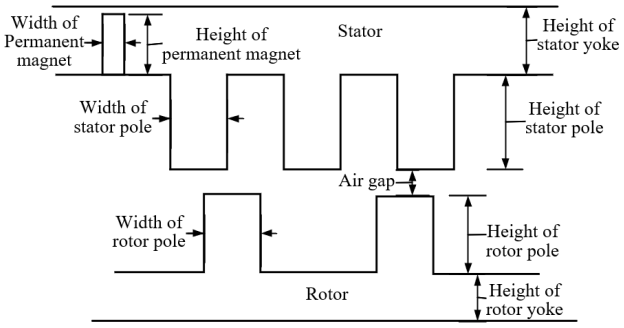

Fig. 2. The structure parameter diagram of 24/16-pole HEDSM

The structure of the 24/16 pole HEDSM is shown in Fig.1, and the structural parameter diagram of HEDSM is shown in Fig.2. The stator and rotor are salient pole slot structure. There are both armature windings and excitation windings on the stator and no windings on the rotor, the coils on the stator teeth are mechanized in series every 45 degrees to form a phase winding. At the same time, four tangential magnetizing permanent magnets are inserted into the stator yoke of the four stator slots respectively, and the magnetizing direction of each permanent magnet is shown in Fig.1.

Meanwhile, the actual utilization area of stator slot with excitation winding and only armature winding is different, in order to ensure that the two stator slots have appropriate slot filling rate, the stator pole of HEDSM adopts the parallel stator pole structure, so that the stator slot embedded with the excitation coil has enough space to place the winding. The parallel slot structure does not change the air gap length and the width of the stator pole, which only makes the magnetic flux path through the stator pole and the stator yoke slightly different, and that does not have a great influence on the electrical characteristics of HEDSM.

B. Mathematical Model of HEDSM

The flux-linkage of HEDSM is built by the phase current, the field current and permanent magnets, which can be expressed by following equation

$$[\Psi] = [L][I] + [\Psi_{pm}] \tag{1}$$

where $[\Psi] = [\Psi_a, \Psi_b, \Psi_c, \Psi_f]^T$, is the flux-linkage of respective phase windings. $[I] = [i_a, i_b, i_c, i_f]^T$, is phase currents vector. $[\Psi_{pm}] = [\Psi_{pa}, \Psi_{pb}, \Psi_{pc}, 0]^T$, is the flux-linkage at null load. $[L]$ is the respective self-inductance and the mutual inductance and

$$[L] = \begin{bmatrix} L_a & L_{ab} & L_{ac} & L_{af} \\ L_{ba} & L_b & L_{bc} & L_{bf} \\ L_{ca} & L_{cb} & L_c & L_{cf} \\ L_{fa} & L_{fb} & L_{fc} & L_f \end{bmatrix} \tag{2}$$

The output torque includes different torque components and can be expressed by

$$T_e = T_k + T_f + T_{pm} \tag{3}$$

$$T_k = \frac{1}{2} i_a^2 \frac{dL_a}{d\theta} + \frac{1}{2} i_b^2 \frac{dL_b}{d\theta} + \frac{1}{2} i_c^2 \frac{dL_c}{d\theta} \tag{4}$$

$$T_f = i_a i_f \frac{dL_{af}}{d\theta} + i_b i_f \frac{dL_{bf}}{d\theta} + i_c i_f \frac{dL_{cf}}{d\theta} \tag{5}$$

$$T_{pm} = i_a \frac{d\Psi_{pa}}{d\theta} + i_b \frac{d\Psi_{pb}}{d\theta} + i_c \frac{d\Psi_{pc}}{d\theta} \tag{6}$$

where T_k is the reluctance torque, which is deduced by the variation of self-inductance with the rotor position. T_f is the excitation torque, which is deduced by the variation of mutual inductance between the armature windings and the excitation windings with rotor position. T_{pm} is the torque generated by permanent magnets.

III. Optimization Design of HEDSM

The basic process of the Taguchi method is mainly divided into the following steps. At first, the optimization parameters and optimization targets need to be determined. Then, the experimental matrix needs to be arranged and the experimental orthogonal matrix needs to be established. After that, the value of each optimization target can be obtained, which is corresponding to each parameter combination in the experimental orthogonal matrix. Finally, the optimization scheme can be obtained by applying some mathematical analysis methods.

A. Initial Structure Design of HEDSM

At present, the main size design of HEDSM refers to the design of asynchronous motors with similar power and similar rated speed. According to experience, the ratio of the shaft length of the doubly salient motor and the outer

diameter of the stator is generally 0.5 to 3.0, and the ratio of the inner diameter to the outer diameter of the stator is generally 0.4 to 0.7, which increases as the number of stator poles increases. Table I is the value of main structural parameters for the 24/16-pole HEDSM, which are designed based on experience.

TABLE I
THE VALUE OF MAIN STRUCTURAL PARAMETERS

Structural Parameter	Value
Stator outer diameter(mm)	304
Stator inner diameter(mm)	202
Rotor outer diameter(mm)	201.2
Rotor inner diameter(mm)	132
Stator pole height(mm)	33
Rotor pole arc (◦)	7.5
Permanent magnet height(mm)	18
Air gap(mm)	0.4
Shaft length(mm)	100
Turns-in-series per pole	120T

B. Optimization Targets and Parameters

Generally, the torque ripple coefficient K_{mb} can be used to evaluate the overall torque ripple degree of the motor, which is expressed by

$$K_{mb} = \frac{T_{max} - T_{min}}{T_{av}} \times 100\% \tag{7}$$

where T_{max} and T_{min} are respectively the maximum and minimum instantaneous torque values in steady state. T_{av} is the average torque value.

Obviously, the average torque T_{av} and torque ripple coefficient K_{mb} are selected as the optimization targets, and it is hoped that the larger the T_{av}, the smaller the K_{mb}, so as to achieve the purpose of optimizing the torque characteristics of the motor.

As is shown in Fig. 2，the flux linkage forms a circuit through the stator yoke, the stator pole, the air gap, the rotor pole, the rotor yoke and the permanent magnet. Therefore, the air gap, stator pole height, rotor pole arc, permanent magnet height and permanent magnet width are selected as optimization parameters. By using Maxwell of Ansys to adjust the optimization parameters repeatedly and verify the simulation, the optimal value range of each optimization parameter can be preliminarily determined, which is shown in Table II.

TABLE II
THE PARAMETER SYMBOL AND VALUE RANGE

Parameter	Parameter symbol	Initial value	Value range
Air gap (mm)	g	0.4	0.30~0.45
Stator pole height (mm)	l_{sp}	33	29~35
Rotor pole arc (◦)	β_r	7.5	7.500~9.375
Permanent magnet width(mm)	b_m	5	5~8
Permanent magnet height(mm)	h_m	18	17~20

Four levels are selected here, and the value of the optimization parameters at each level is shown in Table III.

TABLE III
OPTIMIZATION VARIABLES AND LEVELS

Parameter	g[mm]	l_{sp}[mm]	β_r[◦]	b_m[mm]	h_m[mm]
1	0.30	29	7.500	5	17
2	0.35	31	8.125	6	18
3	0.40	33	8.750	7	19
4	0.45	35	9.375	8	20

C. Orthogonal Experiment

In this paper, the orthogonal array $L_{16}(4^5)$ selected and results calculated by FEM are shown in Table IV. It can be seen that compared with the traditional optimization methods of the motor, which requires $4^5 = 1024$ experiments, the optimization design based on Taguchi method only needs 16 experiments, which greatly reduces the time and improves the efficiency of the optimization design for the motor.

TABLE IV
EXPERIMENTAL MATRIX AND RESULTS OF FEM

No.	Experimental matrix					T_{av}[Nm]	K_{mb}[%]
	g	l_{sp}	β_r	b_m	h_m		
1	1	1	1	1	1	33.93	167.85
2	1	2	2	2	2	38.92	127.47
3	1	3	3	3	3	42.71	112.26
4	1	4	4	4	4	45.02	125.43
5	2	1	2	3	4	38.32	137.18
6	2	2	1	4	3	34.87	169.33
7	2	3	4	1	2	40.20	112.96
8	2	4	3	2	1	39.09	113.32
9	3	1	3	4	2	37.36	108.35
10	3	2	4	3	1	37.61	113.26
11	3	3	1	2	4	31.15	190.56
12	3	4	2	1	3	32.28	141.22
13	4	1	4	2	3	37.22	110.85
14	4	2	3	1	4	36.43	110.84
15	4	3	1	4	2	30.45	148.99
16	4	4	2	3	1	27.59	207.36

D. ANOVA

ANOVA is often used in the analysis of experimental results in the Taguchi method. The role of result analysis is to obtain the optimization scheme. After the analysis of mean and variance, the experimental results of each parameter at different levels can be obtained, and the correlation and degree of influence of parameters on optimization targets can be evaluated, and the optimization scheme can be obtained by comprehensive analysis.

As experimental results are shown in the Table V, it can be known that the mean value of the output torque is 36.70Nm and the mean value of the torque ripple coefficient is 137.33%.

Then the mean value of the simulation results for each optimization target corresponding to each optimization parameter at different levels can be calculated. and the obtained results are shown in the Table V.

TABLE V
THE MEAN VALUE OF THE OPTIMIZATION TARGETS CORRESPONDING TO EACH LEVEL OF EACH PARAMETER

Parameter	level	T_{av}[Nm]	K_{mb}[%]
g	1	40.15	133.23
	2	38.16	133.09
	3	34.61	138.29
	4	32.92	144.51
l_{sp}	1	36.71	131.06
	2	36.96	130.23
	3	36.14	141.15
	4	36.03	146.71
β_r	1	31.90	183.72
	2	34.99	138.72
	3	38.93	111.09
	4	40.01	115.61
b_m	1	35.71	133.22
	2	36.64	135.38
	3	36.56	142.52
	4	36.93	138.01
h_m	1	35.31	135.75
	2	36.01	139.04
	3	36.77	133.42
	4	37.74	140.92

Then the variance and the proportion of each optimization parameter corresponding to each optimization target can be calculated, which can be expressed by

$$SS = \frac{1}{n}\sum_{i=1}^{n}\left(m_{x_i}(S_i) - m(S)\right)^2 \tag{8}$$

where SS is the variance; n is the number of levels; x is the optimization parameter; S is the optimization target; $m_{x_i}(S_i)$ is the mean of S corresponding to each parameter at each level; $m(S)$ is the mean of the optimization targets. And the obtained results are shown in the Table VI.

TABLE VI
THE VARIANCE AND PROPORTION OF EACH TARGET OF EACH OPTIMIZATION PARAMETER

Parameter	T_{av}[Nm]		K_{mb}[%]	
	SS	proportion (%)	SS	proportion (%)
g	6.3305	30.35	21.5740	2.34
l_{sp}	0.4807	2.30	48.7181	5.30
β_r	12.3907	59.42	828.4311	90.14
b_m	0.4702	2.25	11.8717	1.26
h_m	1.1837	5.68	8.4605	0.96
sum	20.8558	100	919.0554	100

According to the above analysis, the air gap and rotor pole arc have great impact on the output torque and the combination of the optimization parameters that can maximize output torque is $g(1)l_{sp}(2)\beta_r(4)b_m(4)h_m(4)$; the rotor pole arc has the greatest impact on the torque ripple and the combination of the optimization parameters that can minimize the torque ripple coefficient is $g(2)l_{sp}(2)\beta_r(3)b_m(1)h_m(3)$. Therefore, the combination of the optimization parameters can be selected as $g(1)l_{sp}(2)\beta_r(4)b_m(2)h_m(3)$. It can be found that the proportion of other parameters is low, making it difficult to make a quick and correct decision.

E. Grey Relational Analysis

GRA is based on the sample data of various factors, and the grey relational coefficients (GRC) is used to describe the strength, size and order of the relationship between factors. Its core is to calculate GRC, that is to establish a reference sequence according to certain rules, take each evaluation object as a comparison sequence, and then dimensionless each sequence to find the correlation between each comparison sequence and the reference sequence, and then draw conclusions according to the magnitude of GRC.

According to GRA, the maximum output torque and the smallest torque ripple are selected as the reference sequences based on the experimental data in Table IV and are denoted as {45.02,108.35}. Since the units of each optimization parameter and optimization target are different, the reference sequence and the control sequence are dimensionless processed by the initial value method, and the reference sequence is processed as {1.3268,0.6455}. According to the grey relational analysis theory, the data obtained by 16 sets of orthogonal experiments are calculated. And then 16 sets of grey relational coefficients (GRC) for the output torque and the torque ripple are obtained.

Since the optimal combination of output torque and torque ripple needs to be taken into account during motor optimization, ρ_1=ρ_2= 0. 5 (ρ is the resolution coefficient, $\rho \in [0,1]$), and the results of the multi-objective mean relational coefficient for each group of experiments are shown in Table VII.

TABLE VII
THE GRC OF EACH OPTIMIZATION TARGET FOR EACH SET OF EXPERIMENTS AND ITS AVERAGE

No.	GRC		mean
	T_{av}	K_{mb}	
1	0.4525	0.4324	0.4425
2	0.6005	0.7033	0.6519
3	0.7989	0.9206	0.8598
4	1.0000	0.7263	0.8632
5	0.5778	0.6112	0.5945
6	0.4745	0.4264	0.4505
7	0.6554	0.9076	0.7815
8	0.6129	0.9088	0.7609
9	0.5448	1.0000	0.7724
10	0.5530	0.9021	0.7276
11	0.3648	0.3561	0.3605
12	0.4184	0.5797	0.4991
13	0.5403	0.9477	0.7440
14	0.5162	0.9481	0.7322
15	0.3861	0.5273	0.4567
16	0.3455	0.3333	0.3394

From the GRA, it can be seen that the degree of correlation between factors and systems depends on the GRC, and the larger the GRC of a parameter, the greater its response to the optimization value of the objective function, and the closer the corresponding target sequence is to the optimal value. The mean GRC of the process parameters at different levels can be calculated by the mean grey relational coefficient of the parameters in Table VII, which are shown in Table VIII.

TABLE VIII
THE MEAN GRC OF THE PROCESS PARAMETERS AT DIFFERENT LEVELS

Level	GRC				
	g	l_{sp}	β_r	b_m	h_m
1	0.7043	0.6383	0.4481	0.6138	0.5969
2	0.6468	0.6405	0.5505	0.6293	0.6263
3	0.5899	0.6146	0.7816	0.6303	0.6383
4	0.5684	0.6156	0.7790	0.6357	0.6376

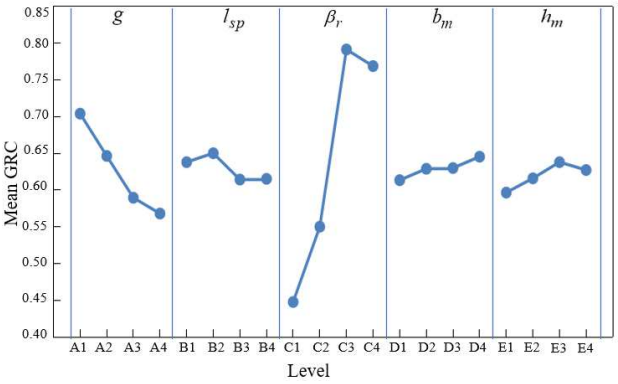

Fig. 3 The mean GRC of each parameter at different levels

According to GRA, the greater the mean GRC corresponding to the level of the parameter, the greater influence the level of the parameter has on the targets. So according to the relational coefficient of each parameter at different levels, as is shown in Fig.3, it is clear in the figure that the levels corresponding to the maximum GRC of each parameter are A1, B2, C3, D4, E3. So, it can be determined that the combination of optimization parameters is $g(1)l_{sp}(2)\beta_r(3)b_m(4)h_m(3)$.

Then the value of optimization targets corresponding to the optimization combinations determined by ANOVA and GRA are calculated separately, which are shown in Table IX. Obviously, compared with ANOVA, GRA results in higher output torque and lower torque ripple of the motor.

TABLE IX
OPTIMIZATION TARGET VALUES CORRESPONDING TO PARAMETER COMBINATIONS FOR DIFFERENT METHODS

	Parameter combinations	T_{av}[Nm]	K_{mb}[%]
ANOVA	$g(1)l_{sp}(2)\beta_r(4)b_m(2)h_m(4)$	43.29	118.95
GRA	$g(1)l_{sp}(2)\beta_r(3)b_m(4)h_m(3)$	44.69	110.19

This can be found out that ANOVA is mainly suitable for single-objective optimization schemes. When in the face of multiple input parameters and multiple targets, the optimal scheme will be selected with certain subjectivity. And the optimization target is complex, it is difficult to judge and obtain the optimal design result quickly. However, GRA can convert multi-objective optimization problems into single-objective optimization problems, which can better optimize parameters of the motor.

Therefore, according to the above analysis, the use of GRA can improve the traditional Taguchi method and the final combination of optimization parameters can be determined as $g(1)l_{sp}(2)\beta_r(3)b_m(4)h_m(3)$.

IV. Simulation Results

According to the previous analysis, the value of parameters for the motor after optimization can be determined, as is shown in the Table X.

TABLE X
THE VALUE OF PARAMETERS FOR HEDSM BEFORE AND AFTER OPTIMIZATION

Parameter	g[mm]	l_{sp}[mm]	β_r[°]	b_m[mm]	h_m[mm]
Initial	0.40	33	7.500	5	18
final	0.30	31	8.750	8	19

In order to verify the effectiveness of the optimization method, a model of HEDSM is established according to the value of parameters after optimization in Maxwell software and the excitation current is set to 10A, the distribution of magnetic field for the motor can be obtained through two-dimensional finite element simulation.

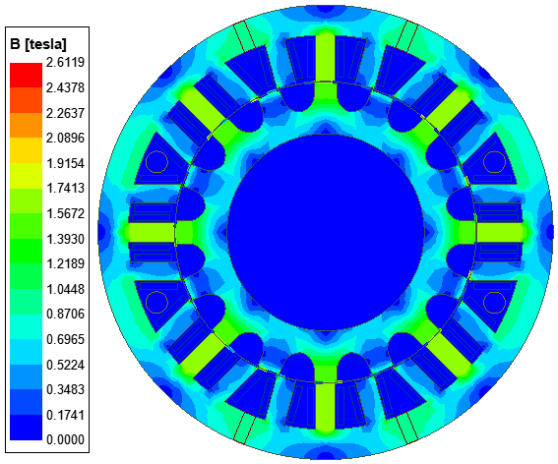

Fig. 4 Magnetic density cloud diagram

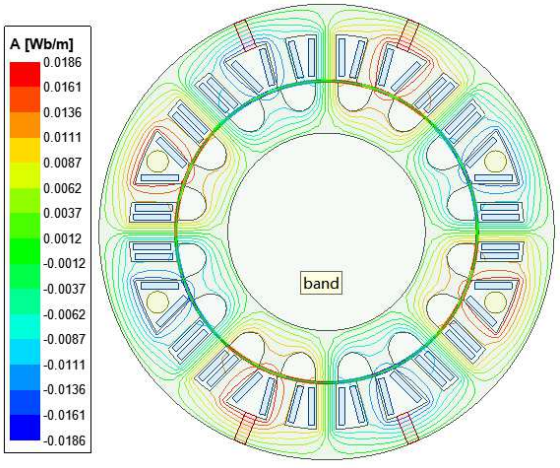

Fig. 5 The distribution of magnetic field

The magnetic density cloud of HEDSM is shown in Fig.4 and the distribution of magnetic field of HEDSM is shown in Fig.5. It can be seen from the figures that the magnetic field distribution of the motor is uniform and the maximum magnetic flux density occurs at the stator pole, which is about 1.8T, which does not exceed the design limit value of 2.0T, which meets the design requirements and effectively avoids magnetic saturation.

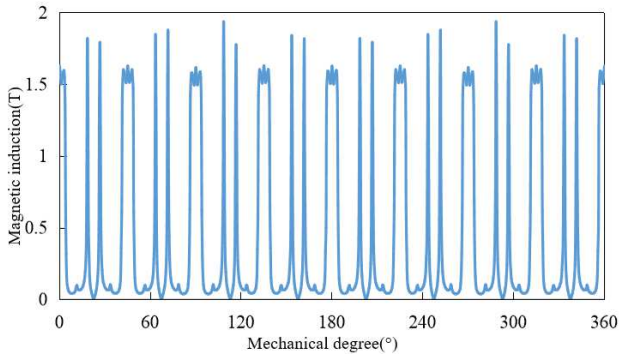

Fig. 6 The distribution of magnetic density at the air gap

Meanwhile, the distribution of magnetic density at the air gap is shown in Fig.6, the distribution of magnetic density at the air gap is also uniform, and its value is about 1.5T.

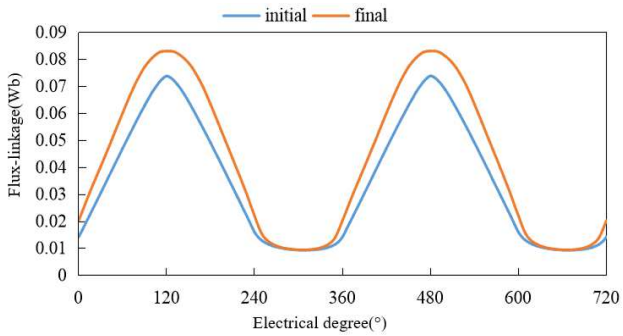

Fig. 7 The flux-linkage of phase B before and after optimization

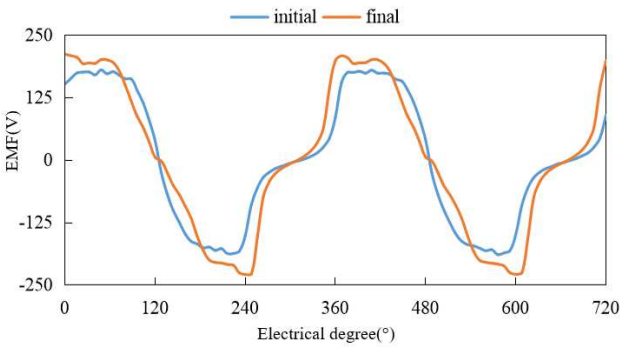

Fig. 8 The back EMF of phase B before and after optimization

Then, the speed of the rotor is set to 2000 rpm and the excitation windings are supplied with rated current. Taking phase B as an example to illustrate the changes of flux-linkage, back EMF and inductance characteristics before and after optimization, the flux-linkage and back EMF curves of phase B for the motor are shown in Fig.7 and Fig.8. As can be seen from the figures, the maximum value of the flux-linkage after optimization increases, and the curve at the maximum value is smoother, because the air gap of the motor is reduced, the magnetic resistance is reduced, the flux-linkage of the motor turn chain increases.

Meanwhile, the increase of the rotor pole arc increases the time when the stator and rotor poles are perfectly aligned, making the curve at the maximum value of the flux-linkage smoother. Due to the increase of the peak-valley value of the flux-linkage, the change rate of the flux-linkage increases, the maximum value of back EMF also increases, and the increase of rotor pole arc increases the transition time at the zero-crossing point of back EMF for the motor.

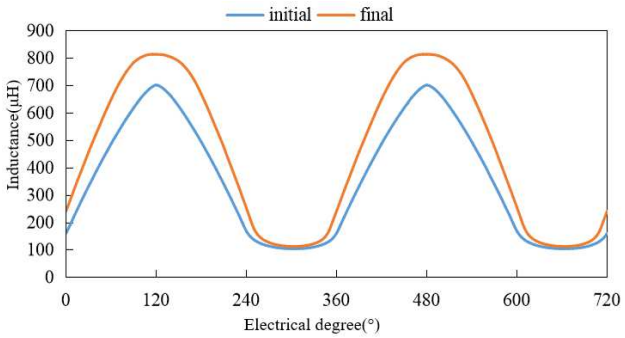

Fig. 9 The inductance curve of phase B before and after optimization

The inductance curve of the phase B of the motor is shown in Fig.9. After optimization, due to the decrease of air gap, magnetic permeability increases, the maximum inductance increases, and the curve at the maximum value is smoother, which is related to the height of stator and rotor pole, stator pole height decreases after optimization, and the minimum value of inductance increases.

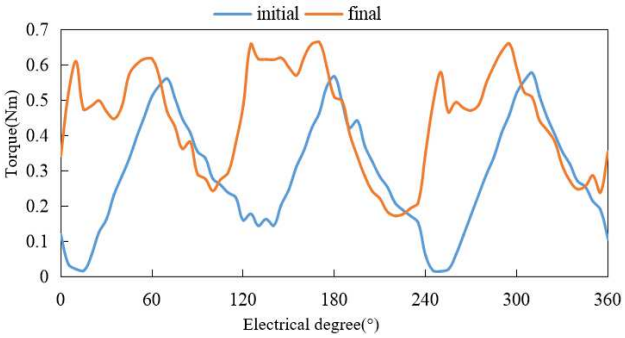

Fig. 10 The electromagnetic torque before and after optimization

Then, a three-phase three-state control method is adopted when the motor operates in electric mode so that the electromagnetic torque of the motor can be obtained. The torque characteristics of the motor before and after optimization are shown in Fig.10. The data of the torque characteristics is shown in Table XI.

After the optimization design of the structure, the average torque of the motor increases by 54.3% from 28.96Nm to 44.69Nm; the torque ripple coefficient reduces by 84.31% from 194.32% to 110.19%. The results show that the motor after optimization has better performance, which verifies the effectiveness of the optimization design.

TABLE XI
THE TORQUE CHARACTERISTICS OF THE MOTOR BEFORE AND AFTER OPTIMIZATION

	T_{av}[Nm]	K_{mb}[%]
Initial	28.96	194.32
After	44.69	110.19

V. Conclusion

Multi-objective optimization design of HEDSM based on Taguchi method is proposed to solve the problem of large torque ripple of HEDSM. With the goal of improving output torque and reducing torque ripple, the structural parameters of a 24/16 pole HEDSM such as the air gap, stator pole height, rotor pole arc, permanent magnet height, and permanent magnet width are optimized.

Meanwhile, because of ANOVA used in the traditional Taguchi method, which is more suitable for single-objective optimization problems, GRA is used to analysis the orthogonal experimental data and the results are compared with the analysis of ANOVA to determine the final optimization parameter combination. After finite element analysis calculation, GRA is found to have better optimization results.

Then, through the two-dimensional finite element simulation, the distribution of magnetic field is uniform and the flux-linkage, back EMF, inductance characteristics and torque characteristics of the motor are better after optimization. It is found that the output torque is improved by 54.3% and the torque ripple coefficient is reduced by 84.31%, which verifies the effectiveness of multi-objective optimization design based on the improved Taguchi method.

In this method, the optimization parameters directly determine effect of the optimization, so how to select the appropriate optimization parameters needs further study.

References

[1] R. Sun, H. Peng, D. Shi, G. Huang and L. Zhuo, "Research on Optimal Design of Commutation Performance of Starter-Generator Used in Aero-Engine," *2021 IEEE International Magnetic Conference (INTERMAG)*, LYON, France, 2021, pp. 1-5.

[2] Z. Zhang, J. Huang, Y. Jiang, W. Geng and Y. Xu, "Overview and analysis of PM starter/generator for aircraft electrical power systems," *in CES Transactions on Electrical Machines and Systems*, vol. 1, no. 2, pp. 117-131, 2017.

[3] Z. Chen, B. Wang, Z. Chen and Y. Yan, "Comparison of Flux Regulation Ability of the Hybrid Excitation Doubly Salient Machines," *in IEEE Transactions on Industrial Electronics*, vol. 61, no. 7, pp. 3155-3166, July 2014.

[4] W. Dai, X. Zhang, C. Cai and Y. Cai, "Control of Hybrid Excitation Doubly Salient Machine with Wide Speed Range," *2018 IEEE International Power Electronics and Application Conference and Exposition (PEAC)*, Shenzhen, China, 2018, pp. 1-5.

[5] Z. Zhang, Y. Tao and Y. Yan, "Investigation of a New Topology of Hybrid Excitation Doubly Salient Brushless DC Generator," *in IEEE Transactions on Industrial Electronics*, vol. 59, no. 6, pp. 2550-2556, June 2012.

[6] Z. Chen, H. Wang and Y. Yan, "A Doubly Salient Starter/Generator with Two-Section Twisted-Rotor Structure for Potential Future Aerospace Application," *in IEEE Transactions on Industrial Electronics*, vol. 59, no. 9, pp. 3588-3595, Sept. 2012.

[7] X. Liu, Z. Chen, J. Zhu and X. Ma, "Researches on the three-phase six-state control strategy of doubly salient electro-magnetic motors", *Proceedings of the CSEE*, vol. 33, no. 12, pp. 138-144, Apr 2013.

[8] Y. Li and C. Mi, "Doubly salient permanent-magnet machine with skewed rotor and six-state commutating mode", *2006 CES/IEEE 5th International Power Electronics and Motion Control Conference*, pp. 1-5, 2006.

[9] C. Hao and R. Nie, "Multi Objective Optimization Design of Dual-Stator Switched Reluctance Motor," *2020 IEEE International Conference on Applied Superconductivity and Electromagnetic Devices (ASEMD)*, Tianjin, China, 2020, pp. 1-2.

[10] J. Liu and Q. Zhou, "Design and Optimization of Permanent Magnet Synchronous Motor Based on Finite Element analysis," *2019 14th IEEE Conference on Industrial Electronics and Applications (ICIEA)*, Xi'an, China, 2019, pp. 2055-2058.

[11] Y. Xia, H. Jiang, X. Yi, Z. Wen and Y. Chen, "Parameter Optimization of Hybrid Excitation Permanent Magnet Synchronous Motor," *2018 21st International Conference on Electrical Machines and Systems (ICEMS)*, Jeju, Korea (South), 2018, pp. 398-401.

[12] A. Purvee and O. Choidorj, "Optimization of Input Values of Simulated Motors Using Grey Relational Analysis," *2021 International Conference on Electrical, Communication, and Computer Engineering (ICECCE),* Kuala Lumpur, Malaysia, 2021, pp. 1-7.